In situ growth and coalescence of He-filled bi-dimensional defects in Si by H supply

M.Vallet[1], J.F. Barbot[1*], E. Oliviero[2], S.E. Donnelly[3], J.A. Hinks[3] and M.F. Beaufort[1]

[1]Institut Pprime (UPR 3346), Department of Material Sciences, CNRS, Université de Poitiers, ENSMA, *BP30179, 86962 Futuroscope Chasseneuil, France*

[2] CSNSM, CNRS - Université Paris-Sud, Bâtiment 108, *Orsay, France*

[3] School of Computing and Engineering, University of Huddersfield, *Huddersfield HD1 3DH, United Kingdom*

[*]Electronic mail: jean.francois.barbot@univ-poitiers.fr

Abstract

In this work, ion implantations with *in situ* transmission electron microscopy observations followed by different rates of temperature ramp were performed in (001)-Si to follow the evolution of He-plates under the influence of hydrogen. The JANNUS and MIAMI facilities were used to study the first stages of growth as well as the interactions between co-planar plates. Results showed that under a limited amount of H, the growth of He-plates resulting from a subcritical stress-corrosion mechanism can be fully described by the kinetic model of Johnson-Mehl-Avrami-Kolmogorov with effective activation energy of 0.9 eV. Elastic calculations showed that the sudden and non-isotropic coalescence of close He-plates occurs when the out-of-plane tensile stress between them is close to the yield strength of silicon. After hydrogen absorption, surface minimization of final structure occurs.

Introduction

Light ion implantation in semiconductors is known to generate, under specific conditions of implantation/annealing, cracks lying parallel to the surface that is used to split the semiconductor and thus to transfer single crystalline thin films onto host substrates. This Smart-Cut technology is widely used in silicon to form silicon on insulator (SOI) structures.[1] The introduction of hydrogen is a necessary step in this thin-film separation. However, the synergy developed by the co-implantation of H and He has been shown to be highly efficient in inducing splitting. Hydrogen implantation results in the formation of tiny planar defects, named H-platelets, and considered as crack precursors.[2] They are filled with molecules of H_2 providing the internal pressure required for the nucleation and growth of defects.[3–5] Hydrogen atoms induce bond-breaking and internal surface passivation.[2,6,7] Helium, on the other hand, does not chemically interact with silicon. Its action is only physical providing a higher internal pressure than H_2 molecules thus enhancing the development and propagation of cracks.[3,8] The co-implantation of hydrogen and helium, thus, allows a reduction in the total fluence of implanted ions and consequently the cost of the SOI structures. More recently it has also been experimentally demonstrated that the introduction of H into specific penny-shaped He-based defects can lead to the propagation and interaction of cracks under particular conditions of annealing, giving rise to the splitting of films.[9] These He-filled two dimensional defects acting as precursors of cracks are referred to as He-plates; they are similar to H-platelets regarding their shape but 10 times larger.[9,10] The processes of exfoliation/blistering are however similar: the high internal pressure of He-plates associated with the embrittlement effect of H cause the coalescence of these nano-sized defects and then the propagation of microcracks in the material.[6,11,12] Very little works have been reported on the crack propagation during thermal annealing, even on the most-studied area of H-platelets in the Smart-Cut process. This is mainly due to the multi-scale nature of the phenomenon. For example, at the nanometer scale, the growth of H-platelets would seem to occur by Ostwald ripening mechanism[13] while at the micrometer scale, the microcracks appear to develop by subcritical stress corrosion by diffusion of H into cracks.[14,15] Reversing the sequence of co-implantation should allow a better understanding of the roles played by the two gases and therefore provide information about the growth processes.

In this study, the first stage of crack propagation was studied through *in situ* transmission electron microscopy (TEM) observations and by using an approach based on successive steps of implantation/annealing of He and H ions. The conditions of He-plate

formation prevent any Ostwald ripening effects by generating a diluted system of defects in the implanted area.[10] The insertion of hydrogen into stable He-plates is thought to trigger the crack propagation through the Si. An advantage of the ion implantation is precise control over the quantity of as-introduced hydrogen. Ion implantations with *in situ* TEM observations were carried out to follow the evolution of He-plates under the influence of hydrogen. Results showed that the growth of He-related plates in their lying planes can be well described by a kinetic model.

Experimental details

At first He-plates must be created. Czochralski grown *n*-type (001) silicon wafers were thus implanted at room temperature (RT) with helium ions at 45 keV to 1×10^{16} cm^{-2}. Implantations were conducted with a controlled current density of 0.5 $\mu A.cm^{-2}$ and with a tilt of 8° to minimize any temperature and channeling effects, respectively. Then a thermal annealing at 350°C for 900 s in high vacuum was performed to form the over-pressurized He-plates. Under such conditions the He-plates are found mainly parallel to the surface.[16] Once created, TEM samples were prepared under two specific configurations, parallel (plan view) or perpendicular (cross-sectional view) to the implanted surface; both being prepared by combining mechanical polishing and argon-milling. Secondly, the as-prepared thin foils were RT implanted with hydrogen ions inside the microscope chamber. The conditions of implantation are listed in Table 1. Figure 1 shows the two configurations that were used either to follow the evolution of isolated single He-plates (the edge-on views facilitate measurement of diameter changes) or to study their interaction over a larger area (the plan view highlights their interactions).

After the H-implantations, the evolution as a function of temperature of the previously-introduced He-plates was studied using *in situ* TEM. Two specific heating rates, 0.2 and 1 K/s, were used to investigate the interaction of H with He-plates. The CSNSM-JANNUS Orsay facility[17] equipped with a FEI Tecnai G^2 20 TEM working at 200 kV and the MIAMI facility[18] in a JEOL 200FX TEM operating at 200 kV were used for this work with somewhat different implantation conditions (energy and angle) in the two facilities, but these parameters do not play any significant role in the evolution of He-plates: the main parameter being the concentration of as-introduced H.

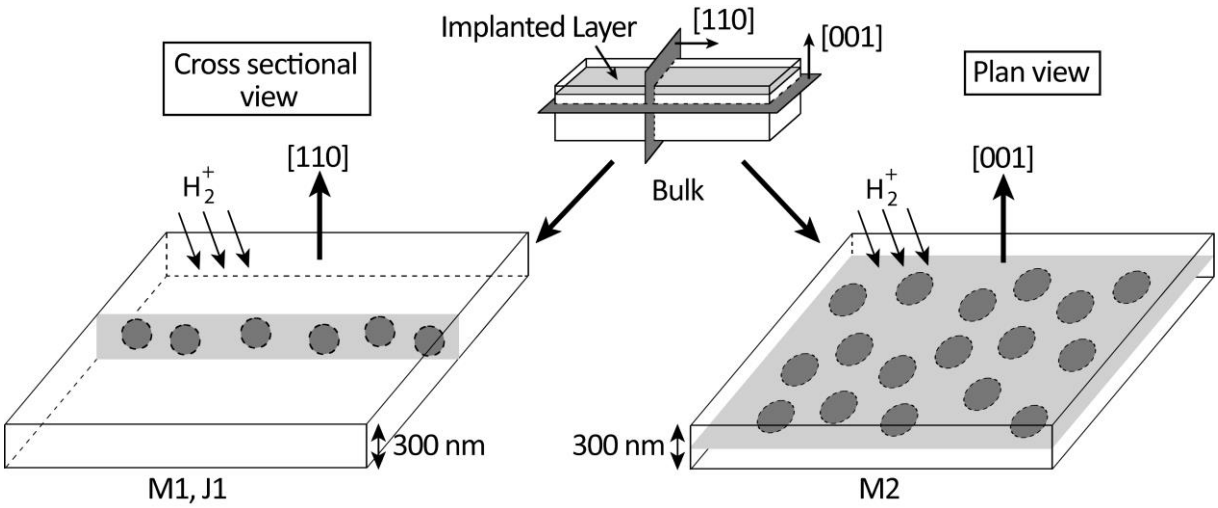

Figure 1. Schematic representation of the two different configurations used for the *in situ* H_2^+-implantations and TEM observations: cross sectional (bottom left) and plan view (bottom right). He-plates were previously introduced by He-implantation at 45 keV ($R_p \approx 380$ nm) to 1×10^{16} cm^{-2} in bulk (001)-Si followed by a 350°C for 15 min anneal.

Sample	M1	J1	M2
Facility	MIAMI	JANNUS	MIAMI
Configuration	Cross-sectional view	Cross-sectional view	Plan view
Fluence (H_2.cm^{-2})	0.5×10^{16}	0.5×10^{16}	1×10^{16}
Implantation parameters	E = 12 keV $\alpha = 30°$	E = 30 keV $\alpha = 45°$	E = 20 keV $\alpha = 30°$
Implantation depth	R_p^{SRIM} = 80 nm	R_p^{SRIM} = 130 nm	R_p^{SRIM} = 115 nm
Ramp rate (β)	1K/s	0.2K/s	1K/s

Table I. Brief description of the various experimental conditions used during this study. Note that the total quantity of implanted ions is lower than the one used in industrial production. The implantation depths were calculated according to SRIM calculations.[19]

Results/Discussion

The thin foils, in cross-sectional or plan view configurations, containing the He-plates were *in situ* H-implanted at RT. During the implantation of H no change in the He-plate microstructure was observed suggesting a limited diffusion of H toward these He-plates even though the coefficient of diffusion is not negligible at RT.[20] However the implantation induced-defects can reduce the diffusion coefficient by trapping phenomena.[21] This trap-

controlled diffusion seems thus to be operative inhibiting any visible change in the He-plate microstructure.

Effect of H on He-plates upon annealing

Figure 2 clearly shows that the contribution of hydrogen (0.5×10^{16} $H_2.cm^{-2}$) strongly modifies the evolution of He-plates with temperature; only the initial and final states at 500°C are presented. As can be seen, the presence of hydrogen induces a substantial growth (of about 50%) of the He-plates during annealing (Fig. 2b) in contrast with the transformation into planetary-like cluster of bubbles observed in the absence of H (Fig. 2c). Such planetary-like clusters are observed during conventional annealing for temperatures higher than 400°C.[10,22,23] These different evolutions appear only for annealing temperatures higher than a critical temperature pointing out the diffusion and H-gettering by the He-plates, so favoring its bi-dimensional growth. These observations agree with dynamical simulations as well as experiments conducted on the disk-shaped defects involving H, for which their growth is controlled by a subcritical stress-corrosion mechanism.[6,24] Moreover, during its planar growth, the He-plate stays over-pressurized due to the formation of H_2 inside the plate. Thus there are two roles of H, a chemical action in breaking Si-Si bonds together with a physical action of internal gas pressure.

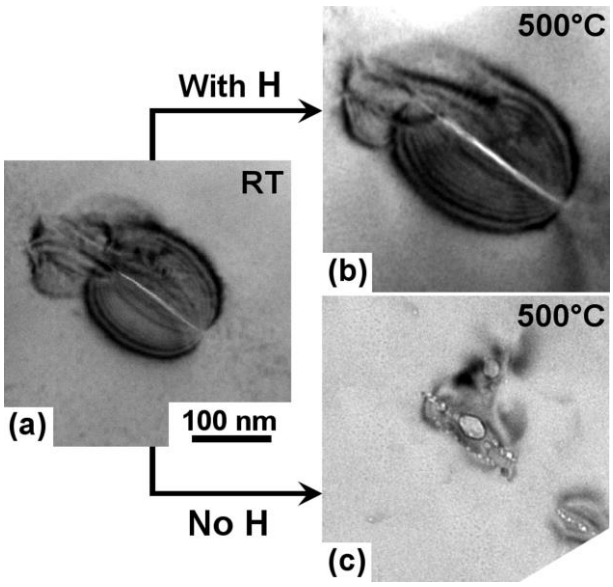

Figure 2. Bright field TEM images of a He-plate observed at RT (a) and after annealing to 500°C with and without contribution of H, (b) and (c), respectively. Figures (a) and (b) show the initial and final evolution of one particular He-plate under similar conditions of observation (the surrounding fringes highlight the strain-related contrast induced by the high gas pressure inside the plates). Scale marker applies to all three micrographs.

Evolution of He-plates with temperature and in the presence of H

The diameter of edge-on He-plates with the contribution of H ($0.5\times10^{16}H_2.cm^{-2}$) was measured throughout the controlled temperature ramp (samples M1 and J1). Figure 3 shows their relative evolution both with the temperature and/or with time. He-plates exhibit a similar behavior. There is first a temperature-range or lag-period for which their diameter does not change. From a critical temperature/time, the diameter increase shows a sigmoidal dependence with a rapid increase of the diameter to reach a plateau. At low rate of ramp rate (0.2 K/s – red curves) the diameter increase becomes significant from about 200°C whereas at a higher rate (1 K/s – black curve) it is at about 300°C. This is consistent with the mechanisms of diffusion previously discussed. During the rapid growth of He-plates the surrounding H is absorbed leading to the decrease of the growth rate and finally no further growth until the end of the experiment. The presence of H at the surface of plate structures modifies the surface free energy and prevents thus any transformation toward a spherical shape.

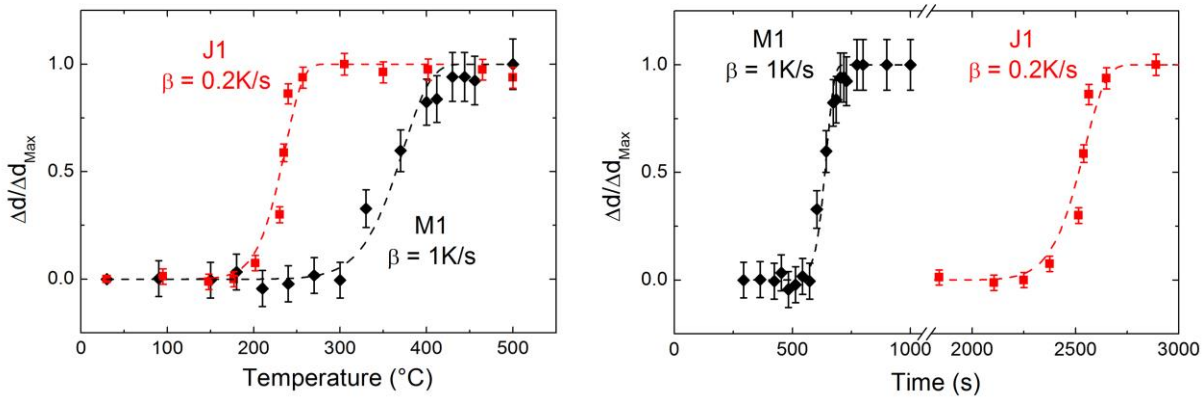

Figure 3. Evolution of the relative diameter of He-plates, during the controlled ramp rate, as a function of the temperature (a) and the time (b). Samples M1 (black) and J1 (red) were implanted with 0.5×10^{16} $H_2.cm^{-2}$ but annealed at different rates of 0.2 and 1 K/s, respectively. Data were fitted using Equation 2.

The evolution of the He-plates as a function of the temperature was analyzed by using the Johnson-Mehl-Avrami-Kolmogorov (JMAK) model extensively used to describe different transformation kinetics as phase transformation and chemical reaction rate from isothermal and non-isothermal considerations.[25–27] Although this model was obtained from the isothermal solution, it constitutes the basis for analyzing non-isothermal experiments. The theory combines nucleation and growth parameters of the transformation to define the volume

fraction of the transformed material χ, as a function of the time, *t*. The general expression of the JMAK equation is:

$$\chi(t) = 1 - \exp\left(-\int_0^t \nu(t,\tau) I(\tau) d\tau\right) \quad (1)$$

where $\nu(t,\tau)$ is the volume of the transformed phase and $I(\tau)$ is the nucleation rate. For a linear rate heating experiment this equation can be simplified and expressed as:

$$\chi(t) = 1 - \exp(-k' t^{2n}) \quad (2)$$

with

$$k'(\beta,T) = k_0' \beta^n \exp\left(-\frac{\Delta H}{k_B T}\right) \quad (3)$$

where β is the heating rate ($\delta T/\delta t$), k_B the Boltzmann constant, ΔH the effective activation energy and *n* the Avrami exponent or order parameter reflecting the dimensionality of the growth. The pre-exponential factor k_0' combines information on nucleation and growth kinetics.

The JMAK model was thus used by setting the relative diameter as a variable of the He-plates $\chi = \Delta d/\Delta d_{max}$. Two parameters govern the transformation kinetics: the nucleation and the growth. As no nucleation of He-plates was observed during the experiments, the transformation kinetic is thus controlled only by the He-plate growth induced by H-diffusion and trapping. The model also considers two different kinds of growth. The first mode describes the growth of precipitates via the addition of external elements from the lattice at the interface. The second mode is mainly based on a growth coming from the initial defect/precipitate itself or controlled by the interface (polymorphic changes, discontinuous precipitation, eutectoid reactions, and interface controlled growth). In our case, H atoms diffuse toward the He-plates and their action induces the growth via the subcritical stress-corrosion mechanism. The second mode of growth is thus more suitable to describe the He-plate evolution under a temperature ramp.

Experimental data were analyzed using the Equation 2 as well as the peak shift method also called Kissinger method adapted for the JMAK model. From the Kissinger plot, the ratio $\Delta H/n$ was estimated to 0.3 eV. However the limited number of experiments with different ramping rate prevents a more accurate determination of this ratio and leads to uncertainties on the values of *n* and ΔH. Experimental curves were then fitted for different combinations of *n* and ΔH with a maximum value of $n = 3$. However, since both experiments were performed by changing the temperature rate only and for an amount of as-introduced H atoms constant, the

k_0' values should not differ (the mechanisms of growth is thus supposed to be not dependent on the temperature ramp rate in the investigated range). According to this additional condition, the best agreement to fit the two curves was obtained for n = 3 and ΔH = 0.9 eV (see Figure 3). A value of n = 3 is usually attributed to a 3D growth while for a 2D growth the Avrami exponent is closer to n = 2.[25] Note that a He-plate is considered as planar defect because its thickness is much smaller than its diameter. But this thickness may affect the transformation kinetics which could explain the experimental Avrami exponent larger than 2. In any case, the limited number of experiments prevents a more-detailed analysis of results.

In situ plan view observations (M2 samples)

Figure 4 exhibits the microstructure evolution of sample M2 during the temperature ramp (1 K/s) up to 500°C. This particular configuration allows a study of the coalescence of He-plates since they lie mainly in planes normal to the electron beam (see Fig.1). Moreover more hydrogen was introduced in order to enhance the growth thus favoring the interaction between He-plates. Only few He-plates, labeled X in Fig. 4, were observed to be in an edge-on orientation and were used in the experiments as reference points. Their increase in size also follows a sigmoidal-type law which is well-described by the JMAK equation (n = 3 and ΔH = 0.9 eV); there is thus no additional mechanism of growth due to the large amount of H. Once again the growth/coalescence of the plan-view He-plates takes place during the rise in temperature, as seen in Fig. 4. Firstly the analysis of TEM pictures (see the dotted lines in Fig. 4) shows that the growth of He-plates, with the addition of H, is not isotropic in their plane. There appears to be preferential growth towards neighboring over-pressurized He-plates probably due to the additive elastic strain fields. Secondly, when some co-planar growing He-plates get sufficiently close (with a sufficiently high strain field) a sudden coalescence occurs without any movement of the individual He-plates. This sudden interaction indicates that the elastic-interaction is sufficient to suddenly break the bonds between the two co-planar approaching plate-edges. This mechanism has also been reported in the interaction of He-filled cracks under the contribution of H.[9,28] Once coalesced, and with no further H-injection, surface modifications are observed toward an ellipsoidal form, presumably to minimize the surface free energy.

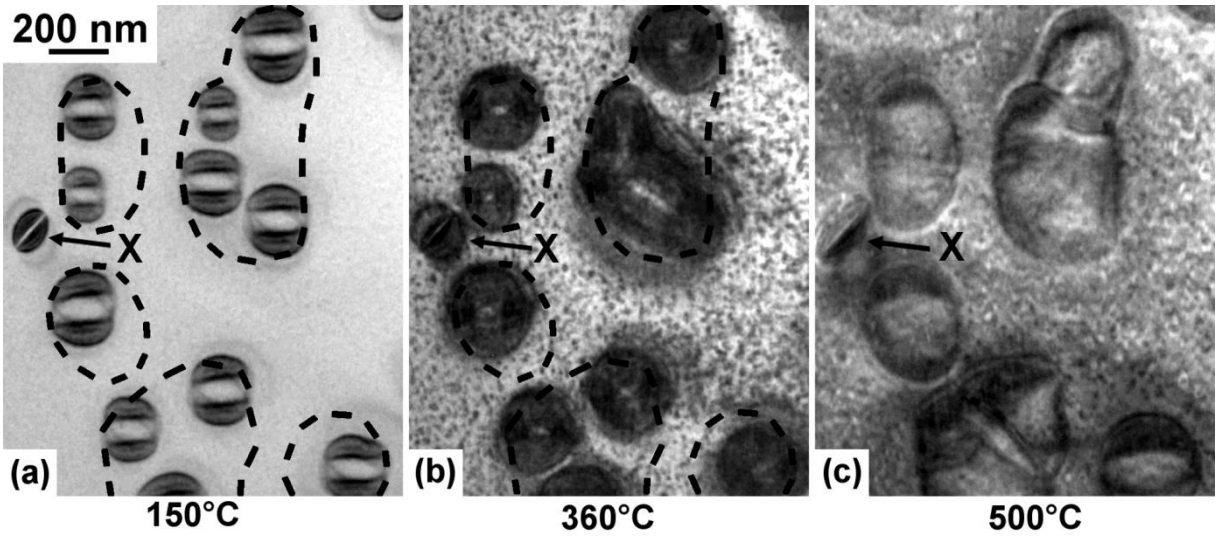

Figure 4. Bright field TEM images of the sample M2 during the thermal annealing up to 500°C. Dotted lines in the figures (a) and (b) report the edges of the final structures observed in (c). Scale marker applies to all three micrographs.

The sudden and isotropic coalescence of close He-related plates results from the high degree of stress between them. To simulate the stress-field induced by a plate, a 2D-model was considered in which a plate is modelled by using two opposite edge dislocations and an effective Burgers vector ($\boldsymbol{b_{eff}}$) to account for the displacement-field introduced by the internal gas pressure. This model was successfully applied to explain the specific arrangements of precipitates under local stresses.[29,30] The stress components were then determined from the Airy stress function φ of an edge dislocation given by:[31]

$$\varphi(x,z) = -\frac{\mu b_{eff}}{2\pi(1-\nu)} x \ln(\sqrt{x^2+z^2}) \qquad (4)$$

where μ is the shear modulus and ν the Poisson's ratio of the material. More details of the method can be found in Reboh *et al.*[30] However, the plates being inside a thin foil of thickness *e*, the free surfaces must be taken into account, this requires that the shear stresses on the surfaces vanish, i.e.:

$$\sigma_{zz}(x,0) = \sigma_{zz}(x,e) = \sigma_{zx}(x,0) = \sigma_{zx}(x,e) = 0 \qquad (5)$$

Figure 5 shows the resulting variations of the out-of plane stress field (σ_{zz}) generated by two plates, 180 nm in diameter, in close proximity embedded in a silicon matrix (depth z = 150 nm) as experimentally observed. Calculations were made for two plates 60 nm from one another, i.e. when instantaneous connection occurred. Note also that calculations were carried out for a depth slightly in front of the plates to suppress any discontinuities of stresses ascribed to edge dislocations. As seen, the region between the two plates is subjected to a

large out-of-plane tensile stress reaching about 6 GPa. This value is close to the theoretical value of the yield strength (7 GPa) of single crystal silicon.[32,33]

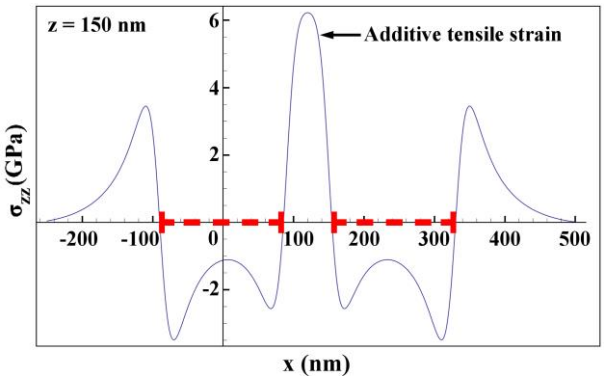

Figure 5. Variation of the out-of-plane stress (σ_{zz}) generated by two plates (180 nm in diameter) with a separation of 60 nm. Plates were modeled by a dipole of edge dislocations (in red) with an effective Burgers vector b_{eff} ≈ 7-8 nm.[30]

Conclusions

A previous study showed that over-pressurized He-plates could be used as precursors for the subcritical propagation of cracks when activated by a diffusional supply of H-atoms.[9] In this work the growth and coalescence of such He-related plates under the influence of H were studied using appropriate experimental conditions of formation and observation. The amount of introduced H was controlled using ion implantation and the TEM observations were conducted *in situ* using the JANNUS and MIAMI facilities. The evolution of plates was studied at two different heating rates. The growth of plates was found to be described by a JMAK model for which the characteristic parameters were determined: the effective activation energy ΔH = 0.9 eV and the exponent n = 3. This model predicts the evolution of the plates under the influence of H with a linear temperature ramp. The sudden coalescence of growing co-planar plates occurs when their edges get sufficiently close. This phenomenon was studied by modelling the plates by a dipole of edge dislocations in a finite solid. Results showed that the coalescence occurs when the out-of-plane tensile stress between two growing plates increases to a value close to the theoretical value of the yield strength of silicon. When all of the H is absorbed, surface minimization mechanisms operate leading to re-arrangements of the structure towards a more symmetrical assembly. This process of successive implantation steps should allow blistering at much lower total fluence than H implantation alone and could thus form the basis of a more-efficient Smart-Cut process.

References

[1] M. Bruel, Electron. Lett. **31**, 1201 (1995)

[2] T. Höchbauer, A. Misra, M. Nastasi, and J.W. Mayer, J. Appl. Phys. **92**, 2335 (2002)

[3] M.K. Weldon, V.E. Marsico, Y.J. Chabal, A. Agarwal, D.J. Eaglesham, J. Sapjeta, W.L. Brown, D.C. Jacobson, Y. Caudano, S.B. Christman and E.E. Chaban, J. Vac. Sci. Technol. B **15**, 1065 (1997)

[4] M.L. David, L. Pizzagalli, F. Pailloux, and J.F. Barbot, Phys. Rev. Lett. **102**, 155504 (2009)

[5] G.F. Cerofolini, F. Corni, S. Frabboni, C. Nobili, G. Ottaviani and R. Tonini, Mat. Sci. Eng. R **27**, 1 (2000)

[6] G. Moras, L.C. Ciacchi, C. Elsässer, P. Gumbsch and A. De Vita, Phys. Rev. Lett. **105**, 075502 (2010)

[7] N. Martsinovich, M.I. Heggie and C.P. Ewels, J. Phys.: Condens. Matter **15**, S2815 (2003)

[8] B. Terreault, Phys. Status Solidi (a) **204**, 2129 (2007)

[9] S. Reboh, J. F. Barbot, M. F. Beaufort, and P. F. P. Fichtner, Appl. Phys. Lett. **96**, 031907 (2010)

[10] P.F.P. Fichtner, J.R. Kaschny, A. Kling, H. Trinkaus, R.A. Yankov, A. Mücklich, W. Skorupa, F.C. Zawislak, L. Amaral, M.F. da Silva and J.C. Soares, Nucl. Instrum. Methods Phys. Res. B **136**, 460 (1998)

[11] L.B. Freund, Appl. Phys. Lett. **70**, 3519 (1997)

[12] C.M. Varma, Appl. Phys. Lett. **71**, 3519 (1997)

[13] J. Grisolia, F. Cristiano, B. De Mauduit, G. Ben Assayag, F. Letertre, B. Aspar, L. Di Cioccio and A. Claverie, J. Appl. Phys. **87**, 8415 (2000)

[14] S. Personnic, K.K. Bourdelle, F. Letertre, A. Tauzin, N. Cherkashin, A. Claverie, R. Fortunier and H. Klocker, J. Appl. Phys. **103**, 023508 (2008)

[15] J.D. Penot, D. Massy, F. Rieutord, F. Mazen, S. Reboh, F. Madeira, L. Capello, D. Landru, and O. Kononchuk, J. Appl. Phys. **114**, 123513 (2013)

[16] M. Vallet, J. F. Barbot, A. Declémy, S. Reboh, and M. F. Beaufort, J. Appl. Phys. **114**, 193501 (2013)

[17] Y. Serruys, M.-O. Ruault, P. Trocellier, S. Henry, O. Kaïtasov and Ph. Trouslard, Nucl. Instrum. Methods Phys. Res. B **240**, 124 (2005)

[18] J.A. Hinks, J.A. van den Berg, and S.E. Donnelly, J. Vac. Sci. Technol. A **29**, 021003 (2011)

[19] J.F. Ziegler, M.D. Ziegler, and J. P. Biersack, "SRIM – the stopping and range of ions in matter (2010)," Nucl. Instrum. Methods Phys. Res. B **268**, 1818 (2010)

[20] S. Fabian, S. Kalbitzer, Ch. Klatt, M. Behar, and Ch. Langpape, Phys. Rev. B **58**, 24 (1998)

[21] T. Zundel and J. Weber, Phys. Rev. B **46**, 2071 (1992)

[22] S. Frabboni, F. Corni, C. Nobili, R. Tonini, and G. Ottaviani, Phys. Rev. B **69**, 165209 (2004)

[23] E. Oliviero, M.F. Beaufort, and J.F. Barbot, Journal of Applied Physics **90**, 1718 (2001)

[24] S. Reboh, A.A. de Mattos, J.F. Barbot, A. Declémy, M.F. Beaufort, R.M. Papaléo, C. P. Bergmann and P. F. P. Fichtner, J. Appl. Phys. **105**, 093528 (2009)

[25] G. Ruitenberg and E. Woldt and A.K. Petford-Long, Thermochim. Acta **378**, 97 (2001)

[26] B. Deb and A. Ghosh, Europhys. Lett. **95,** 26002 (2011)

[27] D.W. Henderson, J. Therm. Anal. Calorim. **15**, 325 (1979)

[28] S. Reboh, J.F. Barbot, M.F. Beaufort and P.F.P. Fitchner, Journal of Physics: Conference Series **281**, 012022 (2011)

[29] S. Reboh, M.F. Beaufort, J.F. Barbot, J. Grilhé and P.F.P. Fichtner Appl. Phys. Lett. **93**, 022106 (2008)

[30] S. Reboh, J.F. Barbot, M. Vallet, M.F. Beaufort, F. Rieutord, F. Mazen, N. Cherkashin, P.F.P. Fichtner and J. Grilhé J. Appl. Phys. **114**, 073517 (2013)

[31] J. P. Hirth and J. Lothe, Theory of Dislocations (Wiley, New York, 1982)

[32] K.E. Petersen, Proceedings of the IEEE **70**, 420 (1982)

[33] X.Q. Feng, Y. Huang, Int. J Solids. Struct. **41**, 4299 (2004)